Discovery of Novel Polycyclic Phloroglucinols via an Improved One-Pot Method

Wentao Zhu, Yichen Tong, Qianyi Feng, Fang Xu,* and Jiyan Pang*

Read Online

ACCESS | 📊 Metrics & More | 📖 Article Recommendations | 🔵 Supporting Information

ABSTRACT: In nature, polycyclic phloroglucinols are a class of compounds with considerable structural diversity and promising biological activities. Herein, we present an improved one-pot method that replaces the solution reaction conditions by mixing the reactants with column chromatography silica gel. Through this convenient, mild, slow, and diversity-oriented strategy, eight structurally unique polycyclic phloroglucinols were discovered, of which compound **1** possesses a rare cage-like skeleton. All compounds determined their structures by X-ray diffraction. Compared with traditional methods, this synthetic strategy produced better diversity and unique structures under milder conditions, suggesting that this method has great potential in lead compound discovery. The optimal reaction conditions were determined by high-performance liquid chromatography (HPLC) monitoring over time. In addition, density functional theory (DFT) calculations were performed to investigate the possible generative pathway of compound **1**. We also examined the neuroprotective actions of selected compounds on SH-SY5Y cells and the MPP⁺-induced *Caenorhabditis elegans* PD model.
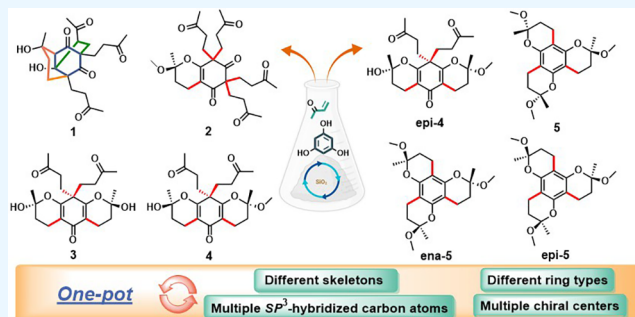
1. INTRODUCTION

Small molecules with complex structures play an essential role in drug research and the exploration of biological systems. Such compounds typically contain dense polycyclic ring systems, multiple stereocenters, and spatially defined arrangements of functional groups.[1] The complexity and three-dimensionality of these molecules allow specific interactions with biological macromolecules and selective modulation of cellular pathways. Compounds in extensive commercial screening collections tend to have fewer stereocenters and more sp²-hybridized carbons, so natural products play a crucial role in the discovery of drug molecules.[2,3] Polycyclic phloroglucinols (PPs), including polycyclic polyprenylated acylphloroglucinols (PPAPs) and polycyclic polymethylated phloroglucinols (PPPs), are attractive research targets for medicinal chemistry research because of their structural diversity and promising biological properties (Figure 1). These compounds are highly regarded for their biological activities, which include anticancer, antibacterial, and anti-viral.[4,5]

In our previous research,[6−10] we identified a series of novel polycyclic phloroglucinols isolated from marine mangrove endophytic fungus from the South China Sea (Figure 1).[11−15] Xyloketal B showed strong L-calcium channel-blocking activities[13] and inhibitory activities of acetylcholine esterase. We also revealed that the xyloketal B analogue (P-53) plays its neuroprotective role by regulating the IRE1/XBP1 signaling pathway.[8] Therefore, synthetic methods and biological

evaluation of novel analogues in the PP family are attractive research areas.[16−18] Grenning et al. reported a synthesis approach for constructing PPAP analogues rapidly through two consecutive Pd-catalyzed reactions, double DcA/Claisen rearrangement, and a DCAA.[17] Cheng et al. developed a new approach to the first asymmetric total syntheses of myrtucommuacetalone, myrtucommuacetalone B, and callistrilones A, C, D, and E, a series of polycyclic polymethylated phloroglucinols (PPPs).[5] The syntheses proceed in 5−7 steps from the building blocks. Although these approaches are efficient and complexity-generating, the synthetic targets are all known skeletons and lack diversity. The discovery of new lead compounds relies on highly divergent structures. Structural complexity and variety are critical for medicinal chemistry and biological evaluation.

Considering that the generation of natural products in nature is slow and mild but diverse, we developed a concise strategy for diversity in this study, inspired by the compound biogenesis pathway. Based on previous research,[19] we added silica gel into the reactive system creatively to replace the
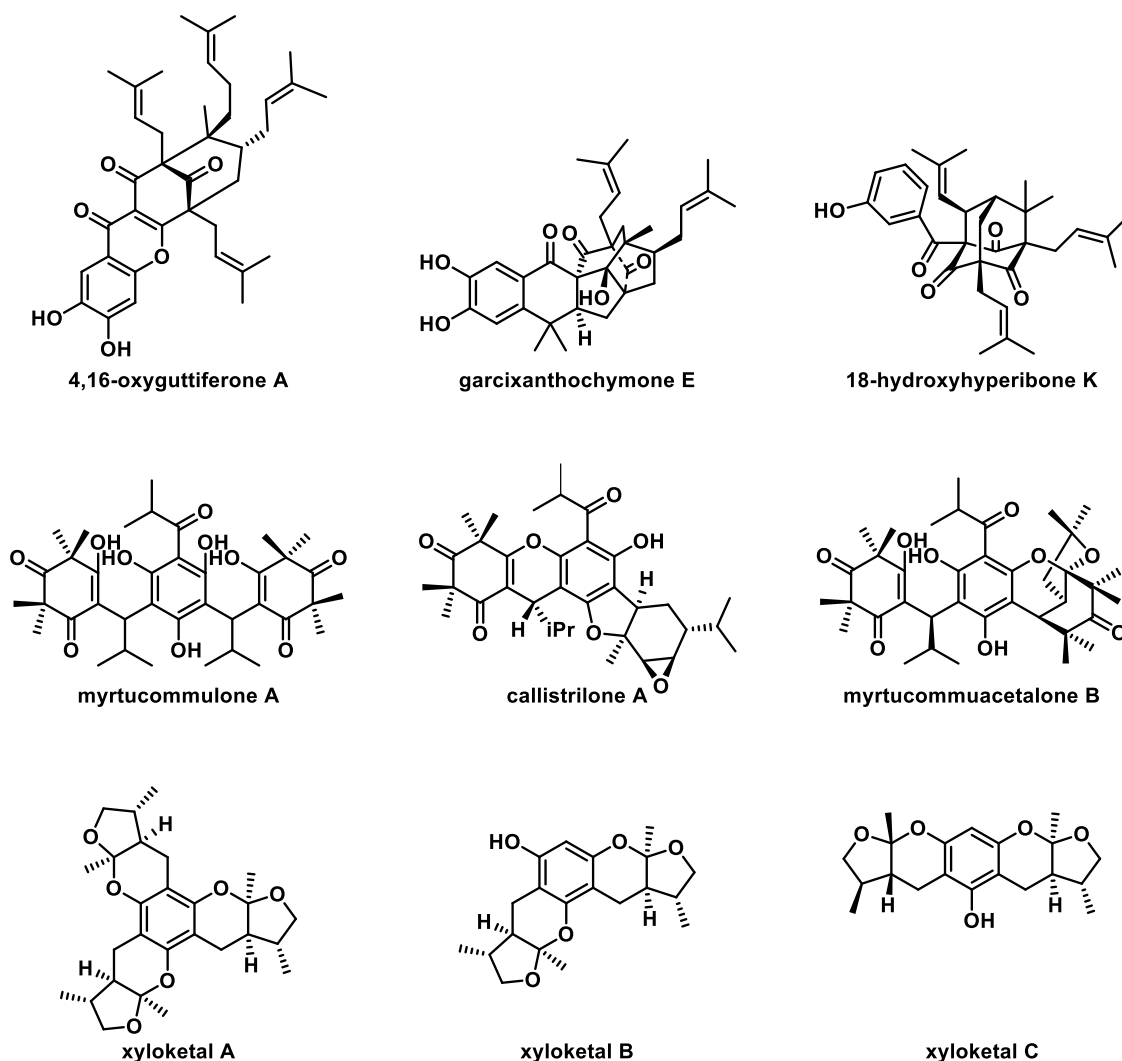
Figure 1. PPAP and PPPs.

solution reaction conditions, which significantly increased the diversity of derivatives. Our approach is more convenient and divergent than the traditional target-oriented synthesis strategy (Figure 2). The generated structures possess different skeletons and ring types, as well as multiple sp³-hybridized carbons and chiral centers that are rare in commercially available compound libraries.

2. RESULTS AND DISCUSSION

2.1. Diversified One-Pot Strategy. To construct complex and structurally diverse polycyclic phloroglucinol derivatives, it was necessary to establish a new convenient method to produce various skeletons. Inspired by the biosynthetic pathway of PPs,[4] we tried to construct diverse polycyclic phloroglucinols using the simplest materials, phloroglucinol (PHL) and methyl vinyl ketone (MVK). Interestingly, we found that mixing the above substrate dissolved in methanol or ethyl acetate in a particular proportion with column chromatography silica gel could generate a series of new derivatives slowly at room temperature for several days. The reaction was monitored by thin-layer chromatography (TLC) and high-performance liquid chromatography (HPLC) and then separated and purified by column chromatography to obtain eight polycyclic phloroglucinol derivatives. The total

isolated yield of compounds under the optimum condition was 57%, and the isolated yields of eight derivatives ranged from 2 to 19%; among them, the yield of compound **1** was the highest, up to 19%.

The eight compounds we obtained are all peculiar in structure, which were the products of intramolecular cyclization after the Michael addition of PHL to 3, 4, or 5 of MVKs, and their features were scarce in natural products (Figure 3). Compound **1** had a rare skeleton with a peculiar cage-like skeleton that had never been reported before. It may be obtained through complex multiple intramolecular additions, and we speculate its generation mechanism through density functional theory (DFT) calculations later. The absolute configuration of compound **1** was determined from a single crystal. Its structure was very complex with a high degree of oxidation and had multiple sp³-hybridized quaternary carbon atoms, which is very different from the molecules in the commercial compound library. Interestingly, compound **1** with the most complex structure had the highest yield in the reaction.

MVK underwent five additions to phloroglucinol followed by intramolecular nucleophilic substitution and methylation to give compound **2**. Compound **3** was obtained by three Michael additions of PHL with MVK, followed by two intramolecular
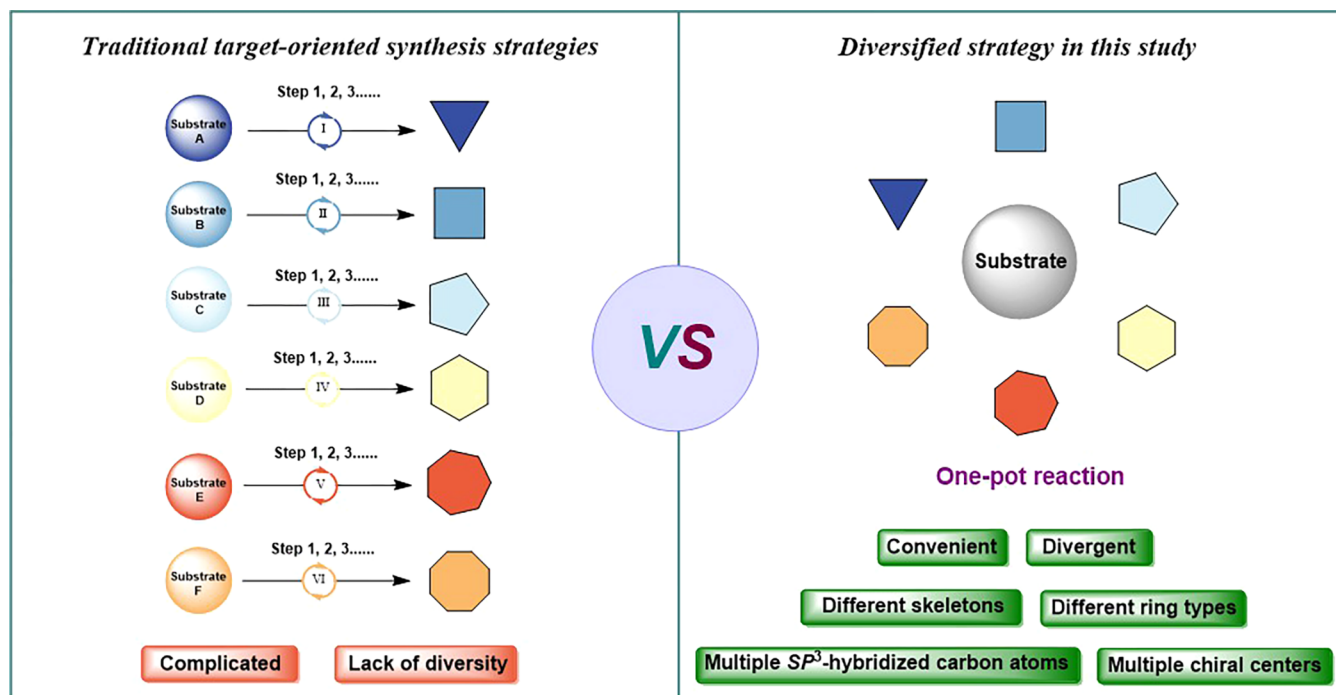
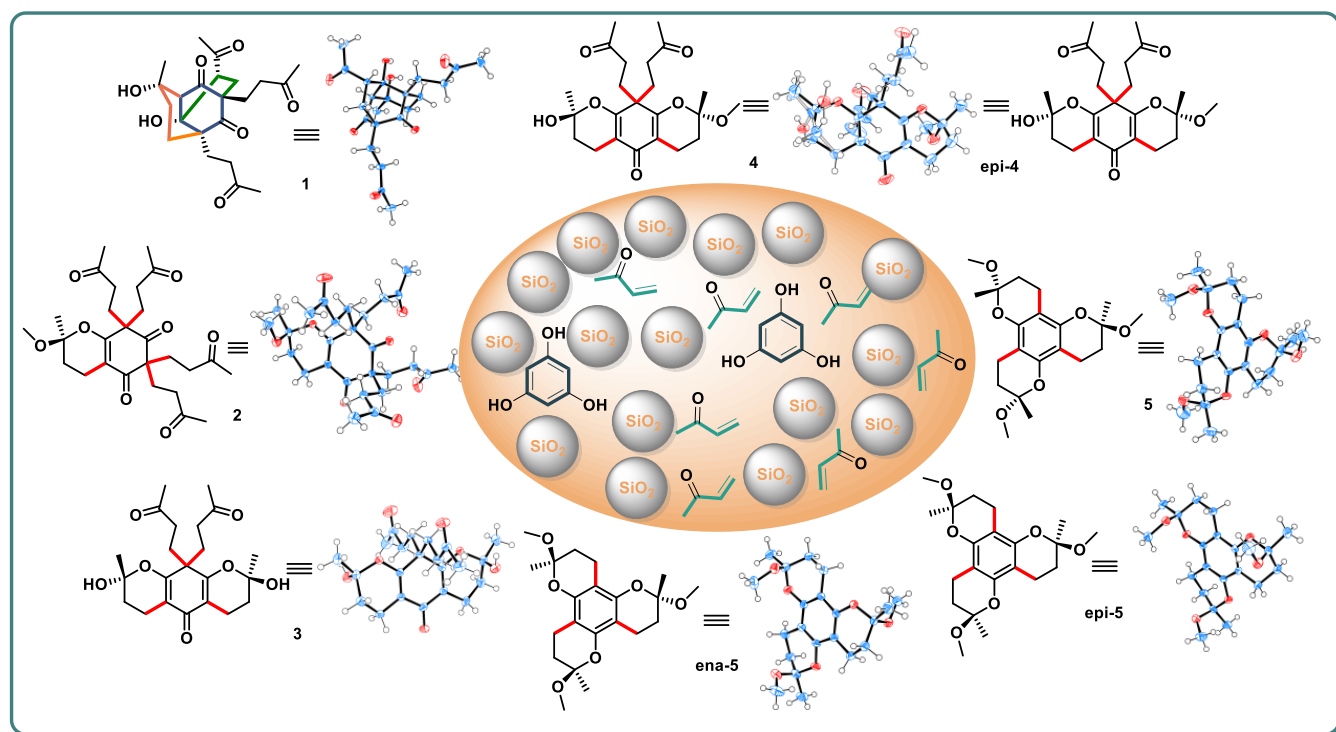**Figure 2.** Traditional target-oriented synthesis strategy versus diversified strategy in this study.

Figure 3. Derivatives of PPs in this study.

nucleophilic additions. Compounds **4** and **epi-4** were the methylation product of compound **3**. Interestingly, these two compounds were a pair of epimers, which are difficult to separate due to their intramolecular hydrogen bonding. We determined the structures by crystallization of the mixture. Compounds **5**, **ena-5**, and **epi-5** had very similar structures. Through a single crystal, we found that compounds **5** and **ena-5** were a pair of enantiomers synthesized in our previous study.[19] Compound **epi-5** is an epimer of **5**, and this unique

distribution of chiral centers is the first to appear in similar natural products. Our previous studies found it challenging to obtain synthetically because of steric hindrance.[7] These products were obtained by one Michael addition of the meso-position of PHL to MVK, followed by three intra-molecular nucleophilic additions of phenolic hydroxyl groups, and then each hydroxyl group was methylated. The unique structure of compound **1** and the inconsistencies of the three chiral centers in compound **epi-5** were extremely rare,
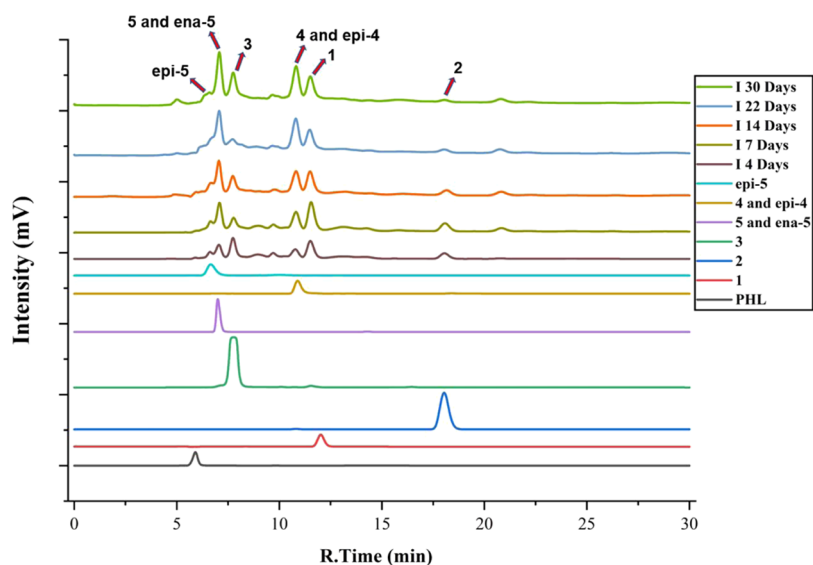
Figure 4. HPLC results of compounds under condition I.

suggesting that our synthetic strategy can synthesize some natural product analogues with complex chiral centers.

It should be noted that in addition to the above structures, several other compounds were also isolated and purified in this reaction system. Still, due to the characteristics of oily compounds, single crystals are difficult to obtain. The NMR spectrum was complex, so it was difficult to determine the structure (maybe a mixture of isomers). We will continue to explore in the future, hoping to obtain more structural types to enrich the application of our strategy.

2.2. Exploring Reaction Conditions. In exploring the reaction conditions, we investigated the solvent, temperature, time reactant ratio, and additive material effect. Sixteen reaction conditions (A−P) groups were designed to track the reaction at different times under HPLC (Table S1).

By comparing the different results of the 16 groups of reaction conditions (Figure S11), we found that the reaction products changed significantly in 3−7 days and reached equilibrium in around 14 days. The ratio of reactants (PHL and MVK) did not considerably affect product diversity. In addition, the participation of methanol was more likely to produce various products than ethyl acetate (conditions A, B, C, and D), probably due to the better nucleophilicity of methanol, and it also showed that the source of hydrogen for proton transfer in the reaction might not be methanol. Additionally, the heated environment yielded the most remarkable diversity and more products (conditions H and I) in less time compared to room temperature.

We further replaced the silica gel with a similar material (column-chromatographic alumina), and similar results were obtained. However, no similar products (such as novel structural compounds **1**, **2**, and so on) were obtained in a solution reaction system simulating acidic conditions with no solid material added (conditions A, F, and G); the yield of compounds in condition G (no solid material added) was only 9%. Few products were found in the solution reaction system tracking by HPLC under condition G, with the lacking diversity indicating that the adsorption of the substrate on the surface of silica gel is a prerequisite for this method, and the role played by silica gel may be complex and multivariate. We also examined the effect of the amount of silica and substrate

equivalents on the reaction, and HPLC results showed that these factors had no significant impact on the reaction rate and yield; isolated yields of compounds in conditions K−P ranged from 27 to 35%, as well as the same type of compounds were detected (Table S1). Therefore, condition **I** (10 mmol PHL and 30 mmol MVK were dissolved in 8 mL of methanol and 8 mL of ethyl acetate, adsorbed on 9 g of silica gel, and reacted at 60 °C) was considered to be a suitable reaction condition with 57% total isolated yield, and a variety of products could be obtained with high efficiency.

Using condition **I** as a reference, we used the compounds under the same chromatographic conditions as a control to clarify the retention times of the significant products in the reaction mixture (Figure 4).

2.3. Exploring the Synthetic Pathway of Compound 1. Compound **1** is an unprecedented derivative with a rare cage-like skeleton. The possible pathways of its generation were more complicated, and we speculated a possible route through the structural characteristics of other products, as shown in Figure 5a. Because of the significance of this compound, we performed density functional theory (DFT) calculations to investigate the formation pathway of intermediates **1−3** to compound **1** in this reaction.

PHL underwent four keto-enol tautomerizations followed by Michael addition to MVK to generate intermediates **1−4**. Then, the cage-like skeleton system was constructed by repeating the process of keto-enol tautomerization, intramolecular nucleophilic addition, and proton transfer twice to obtain compound **1**.

All calculations were performed with the Gaussian 16 program.[20] Geometry optimization of the minimum energy structures and transition states was performed at the B3-LYP level of theory with the 6-31G(d) basis set.[21,22] Harmonic vibrational frequency calculations were performed for all stationary points to determine whether they were local minima or transition structures and to derive the thermochemical corrections for the enthalpies and free energies. Solvent effects in methanol were considered implicitly by performing single-point energy calculations on the gas-phase-optimized geometries using the SMD polarizable continuum mode.[23] Solvation single-point energies were obtained using the 6-
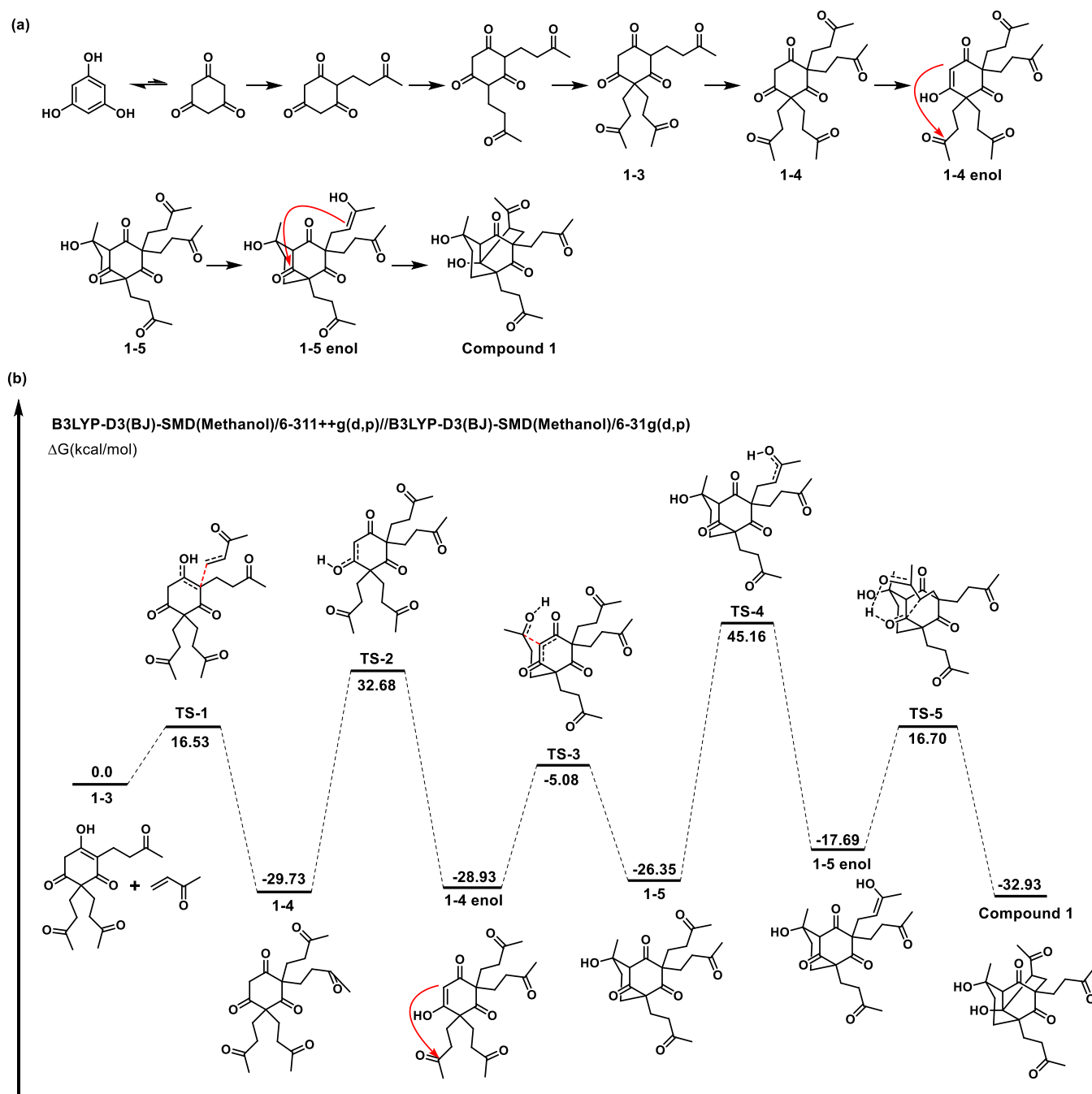
Figure 5. (a) Possible synthetic reaction pathways of compound **1**. (b) Free energy profiles for the possible synthetic pathways of **1**. The values given by kcal/mol are the relative free energies calculated by the 6-311++g (d, p) method in the methanol solvent.

311++G (d,p) basis set, in which dispersion interactions were included. Based on previous theoretical and experimental studies, the proposed reaction pathways of **1** are shown in Figure 5b.

The calculation results further confirmed the presumed formation pathway of compound **1**, and the results showed that the formation of intermediates **TS-2** and **TS-4** needs to cross a higher activation free energy barrier in the reaction pathway of this transformation, which may be the main obstacle to compound **1** in the solution environment.

2.4. Biological Activity. Most natural polycyclic phloroglucinols have a wide range of biological activities. We also found that xyloketal compounds have neuroprotective effects

in our previous work. Therefore, based on the structural similarity, we conducted neuroprotective studies of the compounds.

2.4.1. Neuroprotective Actions on SH-SY5Y Cells. Reactive oxygen species (ROS) play an important role in neurodegenerative diseases, including PD. After dichlorodihydrofluorescein diacetate (DCFH-DA) staining, the intracellular ROS levels of SH-SY5Y cells under the corresponding conditions were measured by fluorescence microscopy. Through preliminary screening, we found that compounds **1**, **4**, and **5*** (**5*** represents a mixture of compounds **5** and **ena-5**) had a neuroprotective effect.
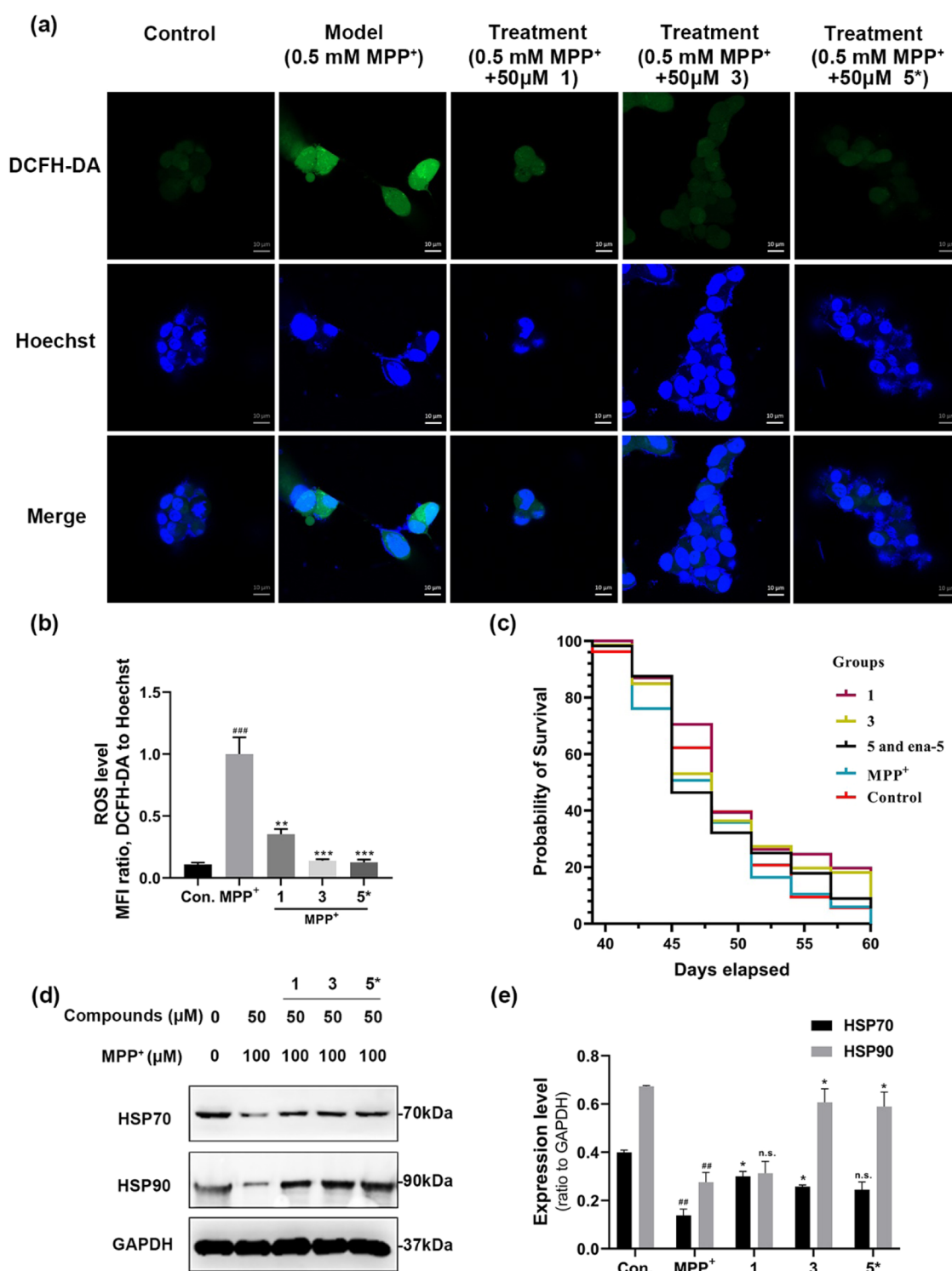
Figure 6. Protective effect of compounds. (a) The ROS levels of SH-SY5Y cells under different conditions were visualized by DCFH-DA straining. Scale bar = 10 μM. (b) Quantitative analysis of the images in (a) showing the ROS levels under corresponding conditions. The ROS levels were determined by the MFI ratios of DAFH-DA to Hoechst. Data represented mean ± standard deviation (SD) (n = 3, number of replicates), and statistical significances were assessed by t-tests (###: $p < 0.005$ vs control group; ***: $p < 0.005$ vs model group; **: $p < 0.01$ vs model group). (c) Survival analysis of **1**, **3**, and **5*** in MPP$^+$-treated *Caenorhabditis elegans* with the Kaplan−Meier method. The survival curve shows the cumulative proportion survival rate in a time-dependent manner. **5*** represents a mixture of **5** and **ena-5**. (d) Western blot analysis showing the expression levels of HSP70 and HSP90 in SH-SY5Y cells treated by MPP$^+$ and compounds. GAPDH was selected as a loading reference. (e) Quantitative analysis of the relative protein expression levels in (c). Data represented mean ± SD (n = 2, number of replicates). Statistical significances were assessed by t-tests (ns: not significant; ##: $p < 0.01$ vs control group; **: $p < 0.01$ *: $p < 0.05$ vs model group).

As shown in Figure 6a,b, the mitochondrial ROS levels of SH-SY5Y cells were inhibited by treatment with different compounds (**1**, **3**, and **5***; $p < 0.005$, 0.005, and 0.01 compared with the model group, respectively). These results suggest that

treatment with derivatives can attenuate MPP$^+$-induced ROS generation.

HSP70 and HSP90 were two molecular chaperones crucial for maintaining the integrity of the proteome in cells.[24−26] To further examine the effect of the derivatives at the protein level, the expression levels of HSP70 and HSP90 were measured by the immunoblot assay. Figure 6d,e shows that both molecular chaperones' expression levels were reduced compared to the model group after treatment with different compounds at 50 μM ($p < 0.05$ vs MPP$^+$). It shows that these compounds may achieve a protective effect by affecting the expression of HSP70 and HSP90.

2.4.2. Neuroprotective Actions Were Examined on the MPP$^+$-Induced C. elegans PD Model. To further verify the neuroprotective effect of these compounds, compounds **1**, **3**, and **5*** were evaluated for their neuroprotective activities in the MPP$^+$-induced *C. elegans* PD model. In *C. elegans*, MPP$^+$ induced DA degeneration dramatically and thus caused death. The survival rates can display the protective results of tested compounds (Figure 6c).

Compounds **1**, **3**, and **5*** showed protection against MPP$^+$-induced toxicity in the MPP$^+$-induced *C. elegans* PD model. ($p < 0.05$, vs MPP$^+$).

3. EXPERIMENTAL SECTION

3.1. Chemistry. All reagents and solvents were of commercial quality and used without further purification. ^{1}H and ^{13}C NMR data were recorded on a Varian Inova 400 M NMR spectrometer operating at 400 and 101 MHz for ^{1}H and ^{13}C, respectively. All chemical shifts were in ppm (δ) with respect to tetramethylsilane (TMS) as an internal standard, and coupling constants (J) were in Hz. Mass spectra were obtained on DSQ (low-resolution mass spectrometer) and MAT95XP (high-resolution mass spectrometer) instruments. The purities (>95%) of all target compounds were checked by HPLC using an LC-2010c with a UV detector.

Samples were injected on a Merck Purospher STAR RP-18e 125 cm 4.6 mm (5 μm) column equipped with a Merck Lichrocart precolumn (Merck, Germany). Analyses were run according to a solvent system (see below). The traces were recorded at 254 nm, and the column temperature was 40 °C. The solvent system consists of a binary system with 0.1% (v/v) aqueous formic acid and acetonitrile 20:80 (v/v), with a flow rate of 0.8 mL/min.

NMR and X-ray data are given in the Supporting Information.

3.1.1. General Synthesis Method. The phloroglucinol, methyl vinyl ketone, solvent, and silica were mixed proportionally in a vessel and left to stand for 4−52 days. After the reaction, ethyl acetate was added, filtered, concentrated under reduced pressure, and purified by column chromatography using petroleum ether and ethyl acetate as the eluant, affording the derivatives.

3.1.1.1. Compound 1. ^{1}H NMR (400 MHz, CDCl$_3$) δ 5.71 (s, 1H), 3.72 (dd, J = 11.2, 3.6 Hz, 1H), 2.72−2.97 (m, 3H), 2.47−2.53 (m, 3H), 2.37 (s, 3H), 2.20 (s, 3H), 2.14 (s, 3H), 2.01−2.12 (m, 3H), 1.59−1.63 (m, 2H) 1.38 (s, 3H), 1.00 (td, J = 14.4,14.4, 4.8 Hz, 1H). ^{13}C NMR (101 MHz, CDCl$_3$) δ 211.9, 211.8, 208.4, 208.2, 202.4, 76.7, 74.8, 65.1 58.5, 53.2, 47.9, 38.4, 38.1, 34.2, 33.5, 30.3, 29.7, 29.4, 29.2, 26.8, 25.7, 21.7. HRMS (ESI, m/z): calculated for C$_{22}$H$_{30}$O$_7$ [M + Na]$^+$ 429.18837, found 429.18793. The title compound was obtained by general synthesis as a white solid in 19% yield.

3.1.1.2. Compound 2. ^{1}H NMR (400 MHz, CDCl$_3$) δ 3.32 (s, 3H), 2.32−2.39 (m, 5H), 2.22−2.30 (m, 9H), 2.11 (d, J = 1.6 Hz, 6H), 2.10 (d, J = 3.6 Hz, 6H), 1.98−2.07 (m, 8H), 1.65 (m, 1H) 1.25 (s, 6H), 0.87 (t, J = 5.2 Hz, 1H). ^{13}C NMR (101 MHz, CDCl$_3$) δ 210.3, 207.0, 206.9, 206.7, 195.5, 166.0, 112.9, 102.0 61.9, 53.9, 53.4, 49.9, 38.5,38.5, 38.4, 38.3, 31.0, 30.1, 30.0, 30.0, 29.9, 29.6, 29.3, 28.6, 22.4, 15.8. HRMS (ESI, m/z): calculated for C$_{27}$H$_{38}$O$_8$ [M + Na]$^+$ 513.24589, found 513.24536. The title compound was obtained by general synthesis as a white solid in 13% yield.

3.1.1.3. Compound 3. ^{1}H NMR (400 MHz, CDCl$_3$) δ 2.84−2.90 (m, 4H), 2.50−2.54 (m, 2H), 2.08−2.19 (s, 8H), 1.95−2.04 (m, 6H), 1.24−1.31 (s, 4H), 1.24−1.31 (m, 4H), 0.90 (t, J = 8.0 Hz, 2H). ^{13}C NMR (101 MHz, CDCl$_3$) δ 214.7, 209.8, 207.9, 186.7, 166.4, 162.5, 115.9, 112.3, 97.7, 48.5, 47.9, 43.6, 38.8, 38.6, 31.0, 30.2, 29.6, 28.0, 16.0, 15.9, 15.4. HRMS (ESI, m/z): calculated for C$_{22}$H$_{30}$O$_7$ [M + Na]$^+$ 429.18837, found 429.18802. The title compound was obtained by general synthesis as a light yellow solid in 11% yield.

3.1.1.4. Compounds 4 and epi-4. ^{1}H NMR (400 MHz, CDCl$_3$) δ 9.24 (s, 1H), 3.26 (d, J = 8.0 Hz, 2H), 2.87 (t, J = 4.0 Hz, 2H), 2.53−2.56 (m, 3H), 2.29−2.47 (m, 4H), 2.12−2.22 (m, 7H), 2.03−2.06 (m, 12H), 1.58 (d, J = 4.0 Hz, 2H), 1.49 (m, 5H). ^{13}C NMR (101 MHz, CDCl$_3$) δ 214.6, 209.1, 209.0, 207.6, 186.5, 186.0, 166.3, 162.4, 162.2, 115.8, 112.8, 112.6, 112.2, 100.3, 97.8, 97.7, 49.4, 47.9, 47.3, 43.6, 38.6, 38.5, 38.3, 38.0,. 37.9, 31.3, 31.0, 30.3, 30.1, 30.0, 29.9, 29.8, 29.7, 29.5, 28.0, 27.9, 22.5, 15.9, 15.3, 15.1, 15.1. HRMS (ESI, m/z): calculated for C$_{23}$H$_{33}$O$_7$ [M + H]$^+$ 421.22208, found 421.22153. The title compound was obtained by general synthesis as a white solid in 7% yield.

3.1.1.5. Compounds 5 and ena-5. HRMS (ESI, m/z): calculated for C$_{21}$H$_{30}$O$_8$ [M + H]$^+$ 379.21152, found 379.21112. NMR data can be found in ref19. The title compound was obtained by general synthesis as a white solid in 5% yield.

3.1.1.6. Compound epi-5. ^{1}H NMR (400 MHz, CDCl$_3$) δ 3.24−3.26 (m, 9H), 2.61−2.68 (m, 6H) 2.02−2.11 (m, 4H), 1.71−1.82 (m, 4H), 1.53−1.54 (m, 9H). ^{13}C NMR (101 MHz, CDCl$_3$) δ 148.2, 148.1, 148.0, 103.0, 102.9, 102.7, 98.2, 49.3, 31.8, 30.1, 23.6, 16.1, 15.9. HRMS (ESI, m/z): calculated for C$_{21}$H$_{30}$O$_8$ [M + H]$^+$ 379.21152, found 379.21115. The title compound was obtained by general synthesis as a white solid in 2% yield.

3.2. Biological Activity. *3.2.1. Cell Culture.* SH-SY5Y cells were cultured with Dulbecco's modified Eagle medium (DMEM, supplemented with 10% fetal bovine serum (FBS) and 1% penicillin−streptomycin solution) at 37 °C in an atmosphere of 5% CO$_2$.

3.2.1.1. Measurement of the Levels of ROS. The ROS levels were measured using dichlorofluorescein diacetate (DCFH-DA) staining. Cells were incubated with 10 mM DCFH-DA at 37 °C for 30 min and then washed with phosphate-buffered saline (PBS) three times. The green fluorescence intensity was determined by high content analysis (scan R, Olympus Life Science Solutions, Waltham, MA) with excitation and emission wavelengths of 488 and 530 nm, respectively.

3.2.2. Worm Strains and Maintenance. All worm strains were obtained from the Caenorhabditis Genetics Center (CGC, 321 Church Street S.E. Minneapolis, MN). Nematodes were cultured in a standard nematode growth medium (NGM)

agar in 60 mm Petri plates and maintained at 20 °C in a temperature-controlled incubator.

Living *Escherichia coli* bacteria (OP50) provided the food source, and 200 μL of bacteria were added to the surface of the NGM plates. The wild-type strain (N2) was used for the longevity-extending assay. The transgenic strain, BZ555 [Pdat-1:GFP], containing the Pdat-1:GFP-linked reporter was used to establish the neuroprotective model and visualize DA neuron expression.

To obtain age-synchronized worms, plates containing worm-laid eggs were washed with M9 buffer and treated using a standard synchronizing protocol of 2% sodium hypochlorite and 5 M sodium hydroxide to dissolve the worms. Then, the eggs were collected via centrifugation, rinsed thrice with M9 buffer, transferred to the surface of the NGM plates, and allowed to hatch in an incubator at 20 °C.

3.2.3. Worm Treatments with MPP$^+$ and Compounds. The experiment was divided into three groups: control group, model group, and treatment group. For the control group, 30 μL of water containing 10% OP50 (v/v) was added to each well of a 96-well plate, and 10 μL of water containing 20 L1 stage larvae and 10 μL of water were added to each well subsequently. For the model group, 30 μL of water containing 10% OP50 (v/v) was added to each well of a 96-well plate, and 10 μL of water containing 20 L1 stage larvae and then 10 μL of 5 mM MPP+ (Sigma-Aldrich, Merck KGaA, Darmstadt, Germany) were added to each well subsequently. The final concentration of MPP$^+$ was 1 mM. For the treatment group, 30 μL of water containing 10% OP50 (v/v) and compounds were added to each well of a 96-well plate, and 10 μL of water containing 20 L1 stage larvae and then 10 μL of 5 mM MPP$^+$ were added to each well subsequently. The final concentration of compounds was 100 μM in 0.1% DMSO. The experiment was conducted based on two strains in parallel.

3.2.4. Longevity-Extending Assay. The worms hatched 48 h after synchronization were transferred to standard NGM plates for pretreatment. The test compounds were diluted in OP50 and added to the surface at a final concentration of 300 μM before incubating overnight at 35 °C. For the control, plates were pretreated with the same amount of DMSO as that used for the drug groups. A total of 30 worms were added to each plate, with two plates for each group. After 24 h, the worms were transferred to new plates pretreated with the test compounds and incubated for 24 h. A total of 50 worms from each group were hatched and transferred to standard NGM plates containing juglone in the agar at a final concentration of 500 μM. Then, the number of dead worms was recorded every hour; each experiment was repeated three times.

3.2.5. Statistics. Experimental data were expressed as mean $\pm$ standard error (SD), and statistical significances between corresponding groups were assessed by *t*-tests. The line charts and column diagrams were generated by GraphPad Prism software (version 8.3.0, GraphPad Software, San Diego, CA), as well as the visualized figure were established with BioRender.com.

4. CONCLUSIONS

In this investigation, a simple and convenient method for finding new structural unique polycyclic phloroglucinol derivatives was developed, in which we added silica gel creatively to replace the solution environment. The most suitable reaction condition with 57% total isolated yield was found through conditional screening under HPLC to generate more diverse derivatives. A series of derivatives with complex structures and multiple chiral centers was synthesized by our method; compounds **1** and **2** with unique structures have relatively high yields, providing more possibilities for the application of this method. The structures of all compounds were determined by X-ray diffraction; the cage-like skeleton of compound **1** never appeared in similar natural products, with a high degree of oxidation and multiple sp^3-hybridized quaternary carbon atoms. The inconsistency of the chiral center of compound **epi-5** was also very rare. In addition, we performed density functional theory (DFT) calculations to investigate the possible pathways of compound **1**. The neuroprotective actions of all compounds were also examined in vitro, and on the MPP$^+$-induced *C. elegans* PD model, compounds **1**, **3**, **5**, and **ena-5** showed moderate protection activity.

In summary, the strategy could easily obtain molecules with excellent structural diversity and potential biological activities. Expanding applications of this method may also have potential in synthesizing other types of natural product derivatives, creating more possibilities for drug discovery and biological research.

■ ASSOCIATED CONTENT

Ⓢ Supporting Information

The Supporting Information is available free of charge at https://pubs.acs.org/doi/10.1021/acsomega.2c06338.

> B3-LYP geometries for all of the optimized compounds (ZIP)

> Supplementary data to this article can be found online at characterization data for all new compounds (PDF)

Accession Codes

CCDC 2204739−2204744 contains the supplementary crystallographic data for this paper. These data can be obtained free of charge via www.ccdc.cam.ac.uk/data_-request/cif, or by emailing data_request@ccdc.cam.ac.uk, or contacting The Cambridge Crystallographic Data Centre, 12 Union Road, Cambridge CB2 1EZ, UK, fax: +44 1223 336033.

■ AUTHOR INFORMATION

Corresponding Authors

Fang Xu − *International Cooperative Laboratory of Traditional Chinese Medicine Modernization and Innovative Drug Development of Chinese Ministry of Education (MOE), Guangzhou City Key Laboratory of Precision Chemical Drug Development, School of Pharmacy, Jinan University, Guangzhou 510632, P. R. China;* ⓞ orcid.org/0000-0002-0895-3071; Phone: +86-020-85220580; Email: xufang@jnu.edu.cn

Jiyan Pang − *School of Chemistry, Sun Yat-Sen University, Guangzhou 510006, P. R. China;* ⓞ orcid.org/0000-0003-0330-2808; Phone: +86-020-8403-6554; Email: cespjy@mail.sysu.edu.cn

Authors

Wentao Zhu − *School of Chemistry, Sun Yat-Sen University, Guangzhou 510006, P. R. China;* ⓞ orcid.org/0000-0003-0433-5935

Yichen Tong − *School of Chemistry, Sun Yat-Sen University, Guangzhou 510006, P. R. China;* ⓞ orcid.org/0000-0001-8561-0526

Qianyi Feng − *International Cooperative Laboratory of Traditional Chinese Medicine Modernization and Innovative Drug Development of Chinese Ministry of Education (MOE), Guangzhou City Key Laboratory of Precision Chemical Drug Development, School of Pharmacy, Jinan University, Guangzhou 510632, P. R. China*

Complete contact information is available at:
https://pubs.acs.org/10.1021/acsomega.2c06338

Notes
The authors declare no competing financial interest.

■ **REFERENCES**

(1) Llabani, E.; Hicklin, R. W.; Lee, H. Y.; Motika, S. E.; Crawford, L. A.; Weerapana, E.; Hergenrother, P. J. Diverse Compounds from Pleuromutilin Lead to a Thioredoxin Inhibitor and Inducer of Ferroptosis. *Nat. Chem.* **2019**, *11*, 521−532.

(2) Swinney, D. C.; Anthony, J. How Were New Medicines Discovered? *Nat. Rev. Drug Discovery* **2011**, *10*, 507−519.

(3) Lovering, F.; Bikker, J.; Humblet, C. Escape from Flatland: Increasing Saturation as an Approach to Improving Clinical Success. *J. Med. Chem.* **2009**, *52*, 6752−6756.

(4) Yang, X.-W.; Grossman, R. B.; Xu, G. Research Progress of Polycyclic Polyprenylated Acylphloroglucinols. *Chem. Rev.* **2018**, *118*, 3508−3558.

(5) Cheng, M.-J.; Cao, J.-Q.; Yang, X.-Y.; Zhong, L.-P.; Hu, L.-J.; Lu, X.; Hou, B.-L.; Hu, Y.-J.; Wang, Y.; You, X.-F.; Wang, L.; Ye, W.-C.; Li, C.-C. Catalytic Asymmetric Total Syntheses of Myrtucommuacetalone, Myrtucommuacetalone B, and Callistrilones A, C, D and E. *Chem. Sci.* **2018**, *9*, 1488−1495.

(6) Zhou, J.-B.; Zheng, Y.-L.; Zeng, Y.-X.; Wang, J.-W.; Pei, Z.; Pang, J.-Y. Marine Derived Xyloketal Derivatives Exhibit Anti-Stress and Anti-Ageing Effects through HSF Pathway in *Caenorhabditis elegans*. *Eur. J. Med. Chem.* **2018**, *148*, 63−72.

(7) Xu, Z.; Li, Y.; Xiang, Q.; Pei, Z.; Liu, X.; Lu, B.; Chen, L.; Wang, G.; Pang, J.; Lin, Y. Design and Synthesis of Novel Xyloketal Derivatives and Their Vasorelaxing Activities in Rat Thoracic Aorta and Angiogenic Activities in Zebrafish Angiogenesis Screen. *J. Med. Chem.* **2010**, *53*, 4642−4653.

(8) Tong, Y.; Mukhamejanova, Z.; Zheng, Y.; Wen, T.; Xu, F.; Pang, J. Marine-Derived Xyloketal Compound Ameliorates MPP[+]-Induced Neuronal Injury through Regulating of the IRE1/XBP1 Signaling Pathway. *ACS Chem. Neurosci.* **2021**, *12*, 3101−3111.

(9) Li, S.; Shen, C.; Guo, W.; Zhang, X.; Liu, S.; Liang, F.; Xu, Z.; Pei, Z.; Song, H.; Qiu, L.; Lin, Y.; Pang, J. Synthesis and Neuroprotective Action of Xyloketal Derivatives in Parkinson's Disease Models. *Mar. Drugs* **2013**, *11*, 5159−5189.

(10) Li, J.; Lu, X.; Wu, Q.; Yu, G.; Xu, Z.; Qiu, L.; Pei, Z.; Lin, Y.; Pang, J. Design, SAR, Angiogenic Activities Evaluation and Pro-Angiogenic Mechanism of New Marine Cyclopeptide Analogs. *Curr. Med. Chem.* **2013**, *20*, 1183−1194.

(11) Wu, X.; Liu, X.; Jiang, G.; Lin, Y.; Chan, W.; Vrijmoed, L. L. P. Xyloketal G, a Novel Metabolite from the Mangrove Fungus Xylaria Sp. 2508. *Chem. Nat. Compd.* **2005**, *41*, 27−29.

(12) Xu, F.; Zhang, Y.; Wang, J.; Pang, J.; Huang, C.; Wu, X.; She, Z.; Vrijmoed, L. L. P.; Jones, E. B. G.; Lin, Y. Benzofuran Derivatives from the Mangrove Endophytic Fungus *Xylaria* Sp. (#2508). *J. Nat. Prod.* **2008**, *71*, 1251−1253.

(13) Wu, X. Y.; Liu, X. H.; Lin, Y. C.; Luo, J. H.; She, Z. G.; Houjin, L.; Chan, W. L.; Antus, S.; Kurtan, T.; Elsässer, B.; Krohn, K. Xyloketal F: A Strong L -Calcium Channel Blocker from the Mangrove Fungus *Xylaria* Sp. (#2508) from the South China Sea Coast: Xyloketal F: A Strong L -Calcium Channel Blocker. *Eur. J. Org. Chem.* **2005**, *2005*, 4061−4064.

(14) Liu, X.; Xu, F.; Zhang, Y.; Liu, L.; Huang, H.; Cai, X.; Lin, Y.; Chan, W. Xyloketal H from the mangrove endophytic fungus Xylaria sp. 2508. *Russ. Chem. Bull.* **2006**, *55*, 1091−1092.

(15) Lin, Y.; Wu, X.; Feng, S.; Jiang, G.; Luo, J.; Zhou, S.; Vrijmoed, L. L. P.; Jones, E. B. G.; Krohn, K.; Steingröver, K.; Zsila, F. Five Unique Compounds: Xyloketals from Mangrove Fungus *Xylaria* Sp. from the South China Sea Coast. *J. Org. Chem.* **2001**, *66*, 6252−6256.

(16) Nishimura, E.; Ohfune, Y.; Shinada, T. Total Synthesis of a Monomeric Phloroglucinol Derivative Isolated from *Myrtus communis*. *Chem. Lett.* **2015**, *44*, 445−447.

(17) Grenning, A. J.; Boyce, J. H.; Porco, J. A. Rapid Synthesis of Polyprenylated Acylphloroglucinol Analogs via Dearomative Conjunctive Allylic Annulation. *J. Am. Chem. Soc.* **2014**, *136*, 11799−11804.

(18) Vita, M. V.; Mieville, P.; Waser, J. Enantioselective Synthesis of Polycyclic Carbocycles via an Alkynylation−Allylation−Cyclization Strategy. *Org. Lett.* **2014**, *16*, 5768−5771.

(19) Xu, Z.; Li, Y.; Lu, B.; Pang, J.; Lin, Y. An Expedient Approach to the Benzopyran Core: Application to Synthesis of the Natural Products (±)-Xyloketals and (±)-Alboatrin. *Chin. J. Chem.* **2010**, *28*, 2441−2446.

(20) Frisch, M. J.; Trucks, G. W.; Schlegel, H. B.; Scuseria, G. E.; Robb, M. A.; Cheeseman, J. R.; Scalmani, G.; Barone, V.; Petersson, G. A.; Nakatsuji, H.; Li, X.; Caricato, M.; Marenich, A. V.; Bloino, J.; Janesko, B. G.; Gomperts, R.; Mennucci, B.; Hratchian, H. P.; Ortiz, J. V.; Izmaylov, A. F.; Sonnenberg, J. L.; Williams; Ding, F.; Lipparini, F.; Egidi, F.; Goings, J.; Peng, B.; Petrone, A.; Henderson, T.; Ranasinghe, D.; Zakrzewski, V. G.; Gao, J.; Rega, N.; Zheng, G.; Liang, W.; Hada, M.; Ehara, M.; Toyota, K.; Fukuda, R.; Hasegawa, J.; Ishida, M.; Nakajima, T.; Honda, Y.; Kitao, O.; Nakai, H.; Vreven, T.; Throssell, K.; Montgomery, J. A., Jr.; Peralta, J. E.; Ogliaro, F.; Bearpark, M. J.; Heyd, J. J.; Brothers, E. N.; Kudin, K. N.; Staroverov, V. N.; Keith, T. A.; Kobayashi, R.; Normand, J.; Raghavachari, K.; Rendell, A. P.; Burant, J. C.; Iyengar, S. S.; Tomasi, J.; Cossi, M.; Millam, J. M.; Klene, M.; Adamo, C.; Cammi, R.; Ochterski, J. W.; Martin, R. L.; Morokuma, K.; Farkas, O.; Foresman, J. B.; Fox, D. J.; et al. *Gaussian 16*, revision B.01; Gaussian, Inc.: Wallingford, CT, 2016.

(21) Lee, C.; Yang, W.; Parr, R. G. Development of the Colle-Salvetti Correlation-Energy Formula into a Functional of the Electron Density. *Phys. Rev. B* **1988**, *37*, 785−789.

(22) Becke, A. D. Density-functional Thermochemistry. III. The Role of Exact Exchange. *J. Chem. Phys.* **1993**, *98*, 5648−5652.

(23) Marenich, A. V.; Cramer, C. J.; Truhlar, D. G. Universal Solvation Model Based on Solute Electron Density and on a Continuum Model of the Solvent Defined by the Bulk Dielectric Constant and Atomic Surface Tensions. *J. Phys. Chem. B* **2009**, *113*, 6378−6396.

(24) Genest, O.; Wickner, S.; Doyle, S. M. Hsp90 and Hsp70 Chaperones: Collaborators in Protein Remodeling. *J. Biol. Chem.* **2019**, *294*, 2109−2120.

(25) Morán Luengo, T.; Mayer, M. P.; Rüdiger, S. G. D. The Hsp70−Hsp90 Chaperone Cascade in Protein Folding. *Trends Cell Biol.* **2019**, *29*, 164−177.

(26) Klaips, C. L.; Jayaraj, G. G.; Hartl, F. U. Pathways of Cellular Proteostasis in Aging and Disease. *J. Cell Biol.* **2018**, *217*, 51−63.